Hindawi
Modelling and Simulation in Engineering
Volume 2022, Article ID 3873639, 16 pages
https://doi.org/10.1155/2022/3873639

Research Article

Computational Validation of the Best Tuning Method for a Vehicle-Integrated PID Controller

Calequela J. T. Manuel, Max M. D. Santos, Giane G. Lenzi, and Angelo M. Tusset

Federal University of Technology-Paraná (UTFPR), Ponta Grossa, PR, Brazil

Correspondence should be addressed to Angelo M. Tusset; tusset@utfpr.edu.br

Received 14 March 2022; Accepted 8 June 2022; Published 25 June 2022

Academic Editor: Noé López Perrusquia

This paper validates and analyzes the robustness of the proportional-integral-derivative (PID) action controller from an open transfer function that integrates a proportional-integral (PI) action controller to obtain the response of a robust action control during the automatic parking maneuver of a vehicle where the simulations are based on 3 adjustment methods: Ziegler-Nichols (ZN), Chien-Hrones-Reswick (CHR), and Cohen-Coon (CC), and as a result of the computer simulations, it is determined the best performance index of the PID controller represented by mathematical and graphic equations with the help of MATLAB/Simulink software.

1. Introduction

The complexity of developing a robust control system [1, 2] that performs adequately when deployed to a vehicle that takes into account noises, disturbances, and adverse conditions [3–5] is a recurrent task in the automotive industry that is increasingly looking more for better solutions and innovations. For the specific problem of aiding the automatic parking maneuver, it is suitable to apply the PID controller that must follow the designated trajectory [6].

1.1. Proposed Problem. For the problem proposed in Figure 1, the transfer function aggregated by the PI controller and the significant variables of the vehicle system are presented.

Table 1 describes the variables that comprise the transfer function of the vehicle system, which allows the extension to proportional-integral-derivative (PID) action controller validation.

The parameters (values) highlighted in Table 1 are used in the computational simulations [7, 8].

1.2. PID Controller Fundamentals. The industrial proportional-integral-derivative (PID) action controller is a control loop feedback technique widely used in control systems [9]. Feedback control systems [10] are a widely deployed strategy to control the process variable by comparing it to a desired value and applying the resulting difference as an error signal to realize the control output in order to reduce or eliminate the error [11, 12].

The proportional-integral-derivative (PID) controller generates its output proportional to the error (P), proportional to the integral of the error (I, integral term), and proportional to the derivative of the error (D, derivative term), considering the position of the parallel PID controller classic [6, 9, 12]. Equation (1) of the algorithm is described below:

$$u(t) = K_{\mathrm{P}}\, e(t) + K_{\mathrm{P}}\, \frac{1}{T_{\mathrm{I}}} \int e(t)\, dt + K_{\mathrm{P}}\, T_{\mathrm{D}}\, \frac{d}{dt}\, e(t). \quad (1)$$

The block diagram characteristics of the PID controller [12, 13] are represented in Figure 2.

The proportional gain also multiplies the integral and derivative terms; the multiplicative factor (T_{D}) is the time derived from the controller, and the derivative action has the function of anticipating the error resulting from the action of the proportional-integral controller in order to eliminate this potential error that is expected and guarantee the stability of the system in less time [6, 11].

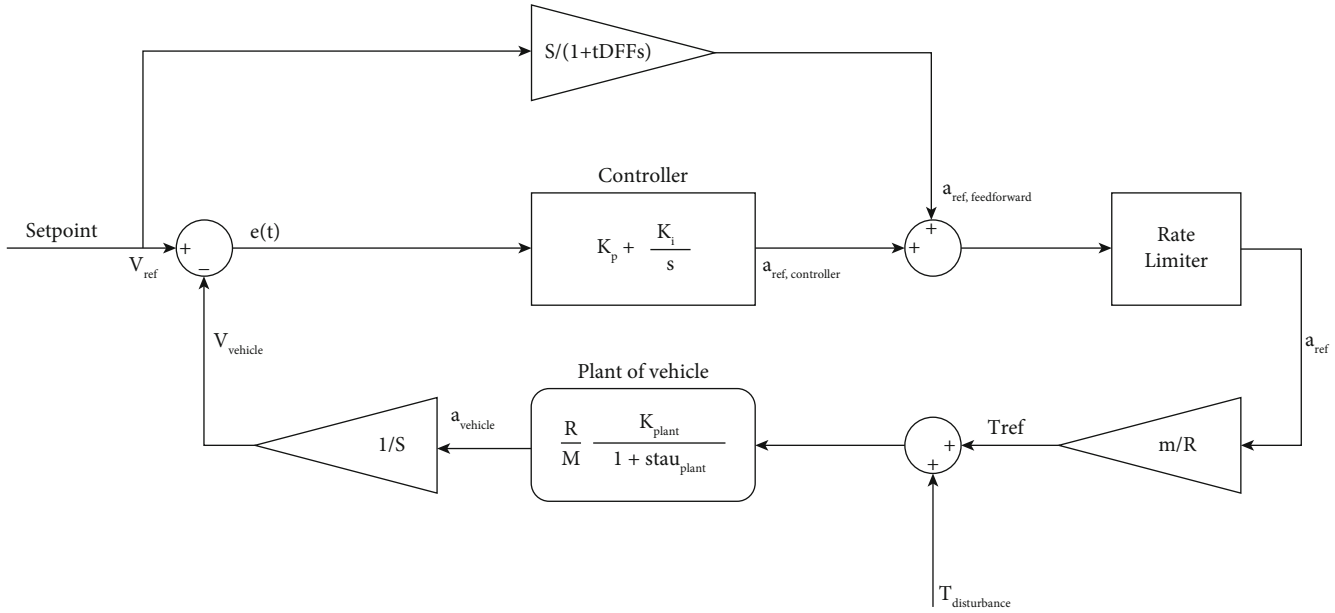

Figure 1: Vehicle block diagram with a PID controller.

Table 1: Block diagram variables.

Variables	Descriptions	Values	Units
m	Mass of the vehicle	2.057	kg
R	Wheel radius	0.3056	m
$\text{tau}_{\text{plant}}$	Time constant	0.10	s
K_{plant}	Static plant gain	1	—
T_{dist}	Torque disturbance	0.1	Nm
V_{vehicle}	Vehicle speed	—	m/s
a_{vehicle}	Vehicle acceleration	—	m/s^2
ref	Reference	—	—
$s/(1 + \text{tDDFs})$	Feedforward term	—	—
$1/s$	Integrative constant	—	—
$e(t)$	System error	—	—
a_{ref}	Reference acceleration	—	m/s^2
T_{ref}	Reference torque	—	Nm

2. Mathematical Modeling

The 3 tuning methods determined to calibrate the PID controller are aimed at evaluating the best system performance index based on the response from the identification of the process frequency (reaction curve).

2.1. Ziegler-Nichols Method. The adjustment method for the PID controller proposed by Ziegler and Nichols [14] is mainly used in industries. This is a manual mode process based on an open-loop step response from a system, and it is indicated for a first-order plant model plus the dead time represented by

$$G(s) = \frac{k}{1 + sT} e^{-sL}, \tag{2}$$

where L is the delay time, T is the time constant, and K stands for the static gain of the controller. If the output of the step response is measured through an experiment, then the parameters K, L, and T (or a, where $a = (KL/T)$) can be extracted from the reaction curve graph. The calculation of the PID controller is based on the results of the reaction curve proposed by Ziegler-Nichols [14, 15], as shown in Table 2.

The values of K_{P}, T_{I}, and T_{D} are $(1.2/a)$, $(2L)$, and $(L/2)$, respectively.

2.2. Chien-Hrones-Reswick Method. Derived from the original Ziegler-Nichols open-loop method, the Chien-Hrones-Reswick (CHR) method gives a faster response without overshoots and also with 20% [16, 17]; the adjustment parameters are based on Table 3.

This method has the ability to adjust the set point and the disturbance. To tune the controller according to the CHR method, L and T parameters must be set [16].

2.3. Cohen-Coon Method. The Cohen-Coon (CC) tuning technique [18] of the PID controller is based on the Ziegler-Nichols method. The Ziegler-Nichols method presents a slow response at a steady state, whereas the Cohen-Coon tuning method can overcome this limitation in the parameter values for adjusting the PID controller [18, 19] based on Table 4.

This method takes the parameters of the PID controller and tries the open-loop transfer function. If there is a long delay in the process in relation to the open-loop time constant, it presents a better answer about the Ziegler-Nichols method, and the three initial adjustment parameters are as

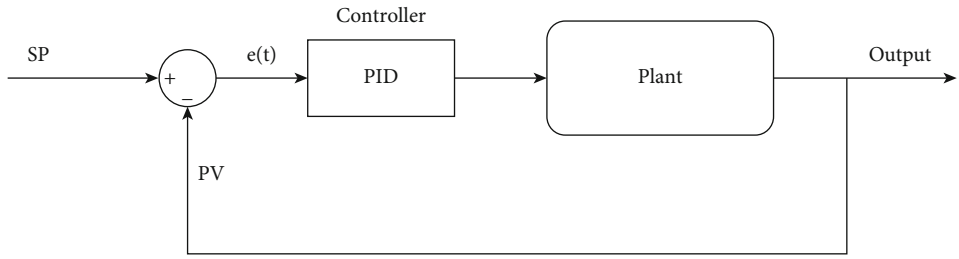

Figure 2: PID controller features.

Table 2: Controller parameters for the Ziegler-Nichols method.

Controller type	K_P	T_I	T_D
P	$\frac{T}{KL}$	∞	0
PI	$0.9\frac{T}{KL}$	$\frac{L}{0.3}$	0
PID	$1.2\frac{T}{KL}$	$2L$	$0.5L$

follows: steady output state (K), effective time constant of the first-order response (s), and dead time (t) [20, 21].

3. Experimental Data Used in PI Controller Simulation

From the block diagram proposed in Figure 1, the exit speed and acceleration of the vehicle are estimated, and an approach and simplification for the study of the transfer function associated with the PI controller [22] responsible for controlling the plant of a given vehicle are determined. The plant's open-loop [23] acceleration transfer function is referred to as $G_{(s)}$, according to

$$G_{(s)} = \left(\frac{m}{R} + T_{\text{dist}}\right)\left(\frac{R}{m}\frac{K_{\text{plant}}}{1 + s\,\text{tau}_{\text{plant}}}\right). \tag{3}$$

Using the MATLAB software [24] and replacing the values in Table 1 in the plant transfer function, the resolution of the transfer function description in Equation (4) is presented:

$$G_{(s)} = \frac{1.003}{0.1\,s + 1}. \tag{4}$$

The current simulator is controlled by a proportional-integral (PI) action designed with minimum proportional gain ($K_{\text{Pmini}} = 2$) and minimum integrative gain ($T_{\text{Imini}} = 1$) and maximum proportional gain ($K_{\text{Pmax}} = 2$) and maximum integrative gain ($T_{\text{Imax}} = 3$). The plant operates with minimum gain ($K_{\text{plant}} = 1$) and maximum gain ($K_{\text{plant}} = 3$). The open-loop acceleration transfer function [25] after the step signal is applied has the following behavior, as shown in Figure 3.

The first step was to consider all the minimum values of the plant in the open loop and the PI controller gain, as shown in Figure 3.

The resolution was presented by MATLAB [26], where the PI controller obtained the following transfer function, according to

$$G_{\text{P}(s)} = \frac{2s + 2}{s}. \tag{5}$$

The output variables do not track input variables; however, the system is not controlled by the proposed proportional-integral (PI) controller output that does not have the desired gain. When considering a closed loop, the acceleration and velocity [27] responses are, respectively, shown in Figure 4.

The acceleration (Figure 4(a)) shows a fast output signal in relation to time, but at no time is it stable. This directly influences the behavior of the velocity signal (Figure 4(b)); therefore, it does not guarantee any stability in the system.

The second step was to consider all the maximum values of the gain of the plant and the PI controller: in this case, the open-loop transfer function [28] is represented by

$$G_{(s)} = \frac{3.003}{0.1\,s + 1}. \tag{6}$$

The open-loop acceleration transfer function after the step signal [29] is applied has the following behavior, as shown in Figure 5.

The resolution was presented by MATLAB, where the PI controller [30] obtained the following transfer function, according to

$$G_{\text{P}(s)} = \frac{6s + 2}{3s}. \tag{7}$$

When considering a closed loop, the acceleration and velocity responses are, respectively, shown in Figure 6.

The output variables do not track input variables; however, the system is not controlled by the proposed proportional-integral (PI) controller output that does not have the desired gain.

3.1. Considerations. In this case, the output of the closed-loop PI controller is similar to that of the open-loop system response for the minimum and maximum gains of the controller, as shown in Figures 3–6; the acceleration (Figure 6(a)) does not present an adequate output, with sudden changes in relation to time. The speed (Figure 6(b)) is

Table 3: Controller parameters for the Chien-Hrones-Reswick method.

Controller type	With 0% overshoot			With 20% overshoot		
	K_P	T_I	T_D	K_P	T_I	T_D
PID	$\frac{0.6}{a}$	T	$0.5L$	$\frac{0.95}{a}$	$1.4T$	$0.47L$

Table 4: Controller parameters for the Cohen-Coon method.

Controller type	K_P	T_I	T_D
PID	$\frac{1.35\,T}{KL}\left(1+\frac{0.18\tau}{1-\tau}\right)$	$\frac{2.5-2\tau}{1-0.39\tau}L$	$\frac{0.37-0.37\tau}{1-0.81\tau}L$

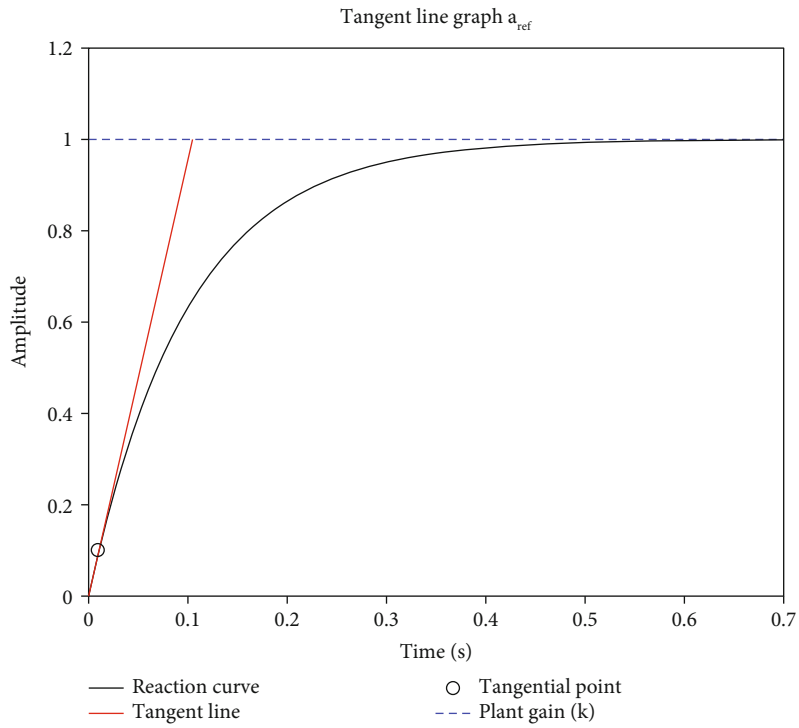

Figure 3: Reaction curve or a_{ref} tangent line in open-loop PI (1).

not constant in relation to the estimated time. Both variables do not perform satisfactorily; this reflects the lack of control of the system.

4. Results: Experimental Data Used in PID Controller Simulation

For proper control of the vehicle plant, the system must be considered a closed loop; the PID controller [31] calculation is based on Table 2 proposed by Ziegler-Nichols (ZN), where the PID controller gains are found, respectively.

4.1. Minimum Plant Gain (ZN). From Equation (3), the minimum plant gain ($K_{plant} = 1$) was replaced together with the parameters of Tables 1 and 2 with the help of MATLAB software; the values of L, tau, and T are obtained; however, the PID controller is represented by

$$G_{P(s)} = \frac{0.001157s^2 + 0.2512s + 13.64}{0.01842s}. \quad (8)$$

The PID controller output can be evaluated by the reaction curve method; the system is excited by a step input signal, as shown in Figure 7.

The output of the PID controller (reference acceleration) starts to be identified from the amplitude (gain $K = 0, 5$). At gain $K = 1$, the controller output has an overshoot and a low stationary error, and at time 0.1 s, the system starts to stabilize. The acceleration response and vehicle speed, respectively, are shown in Figure 8.

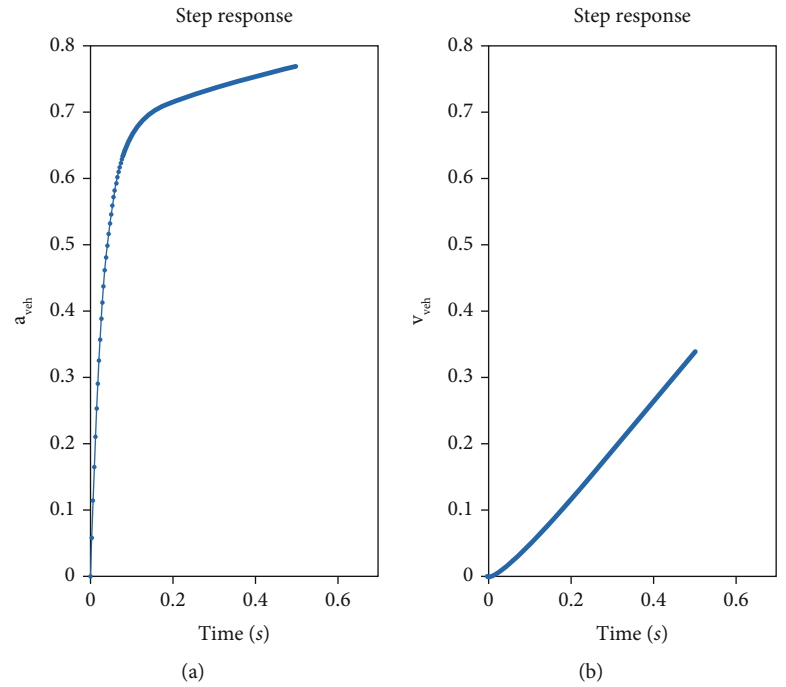

FIGURE 4: Vehicle acceleration (a) and velocity (b) responses, respectively, in PI (1).

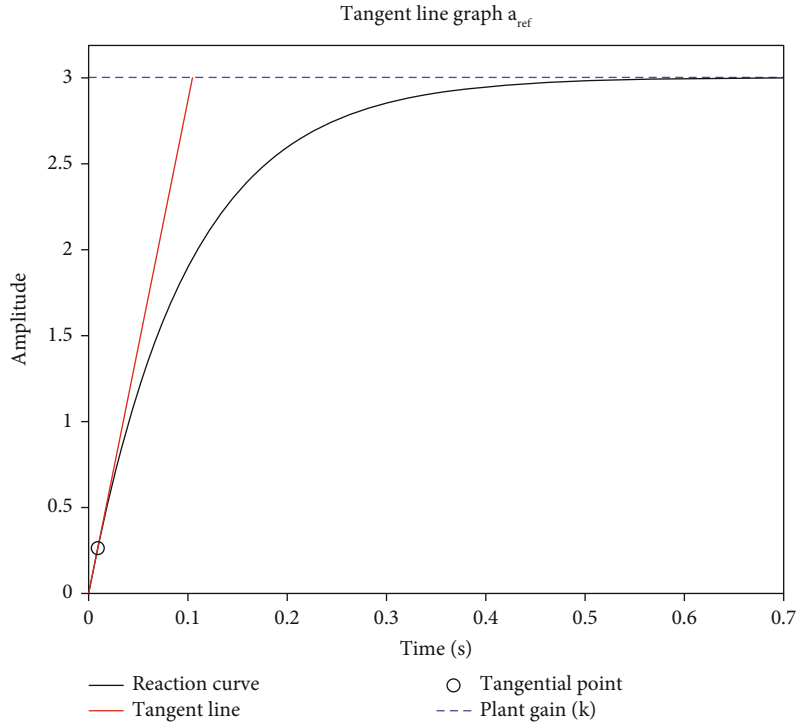

FIGURE 5: Reaction curve or a_{ref} tangent line in open-loop PI (3).

Compared to the response of the PI controller, the results of the PID controller are better and guarantee stability in the system.

4.2. Maximum Plant Gain (ZN). From Equation (3), the maximum plant gain ($K_{plant} = 3$) was replaced together with the parameters of Tables 1 and 2 with the help of MATLAB software; the values of L, tau, and T are obtained; however, the PID controller is represented by

$$G_{P(s)} = \frac{0.0003855s^2 + 0.08374s + 4.547}{0.01842s}. \quad (9)$$

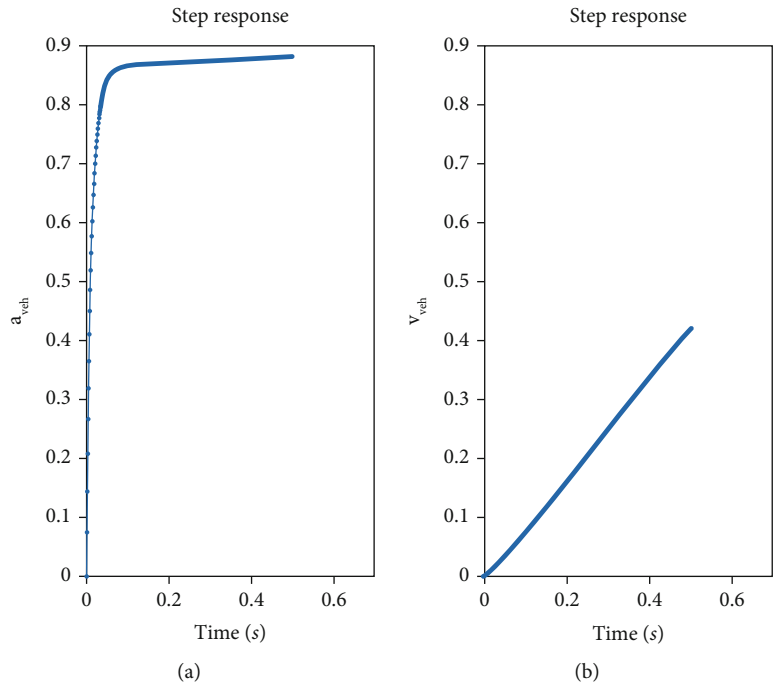

Figure 6: Vehicle acceleration (a) and speed (b) responses, respectively, in PI (3).

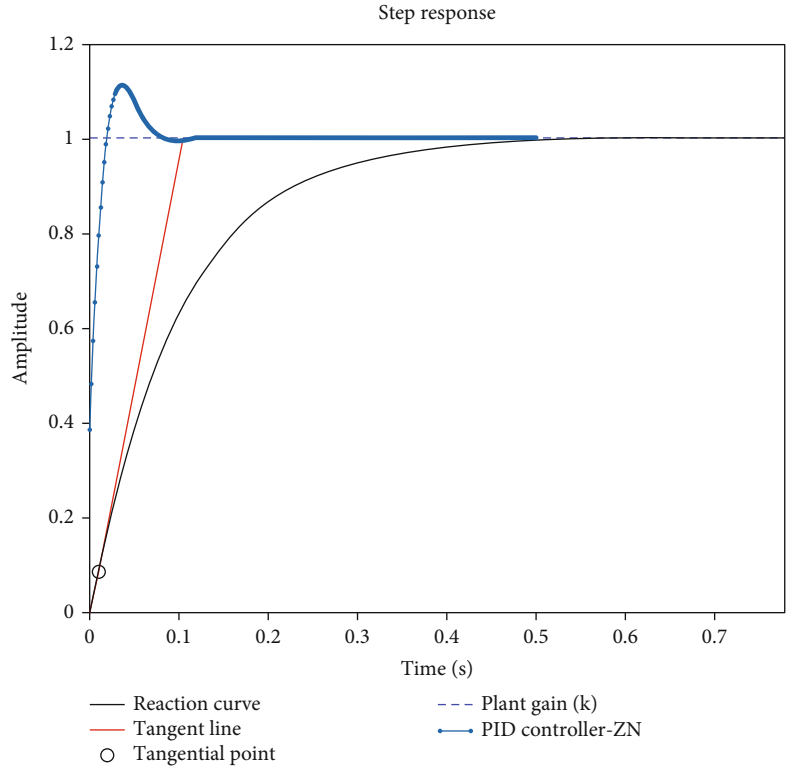

Figure 7: Reaction curve or a_{ref} tangent line in closed-loop PID-ZN (1).

The PID controller output can be evaluated by the reaction curve method; the system is excited by a step input signal, as shown in Figure 9.

The PID controller output signal (reference acceleration) does not reach the desired gain ($K = 3$) to stabilize the system; in this case, it produces a large stationary error [32,

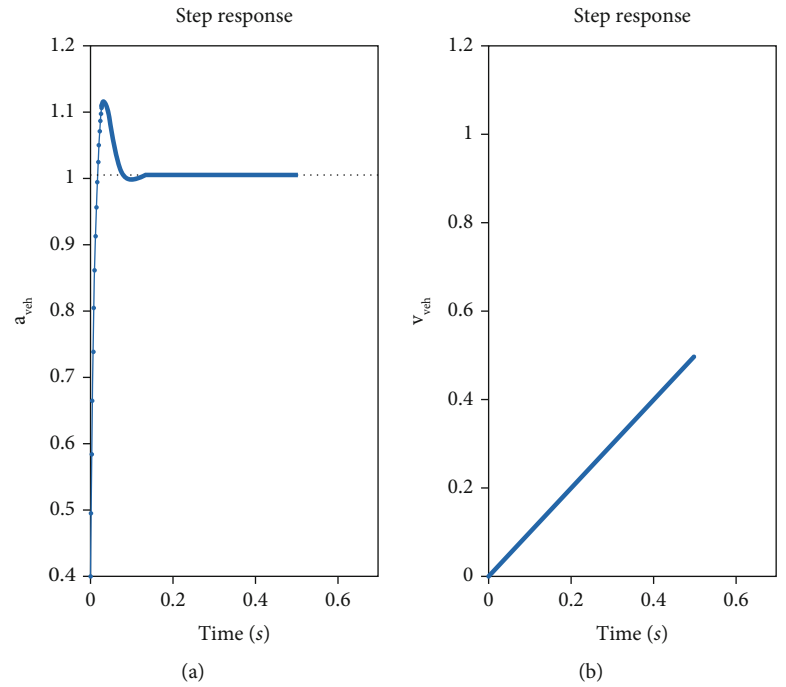

Figure 8: Acceleration (a) and vehicle velocity (b), respectively, in closed-loop PID-ZN (1).

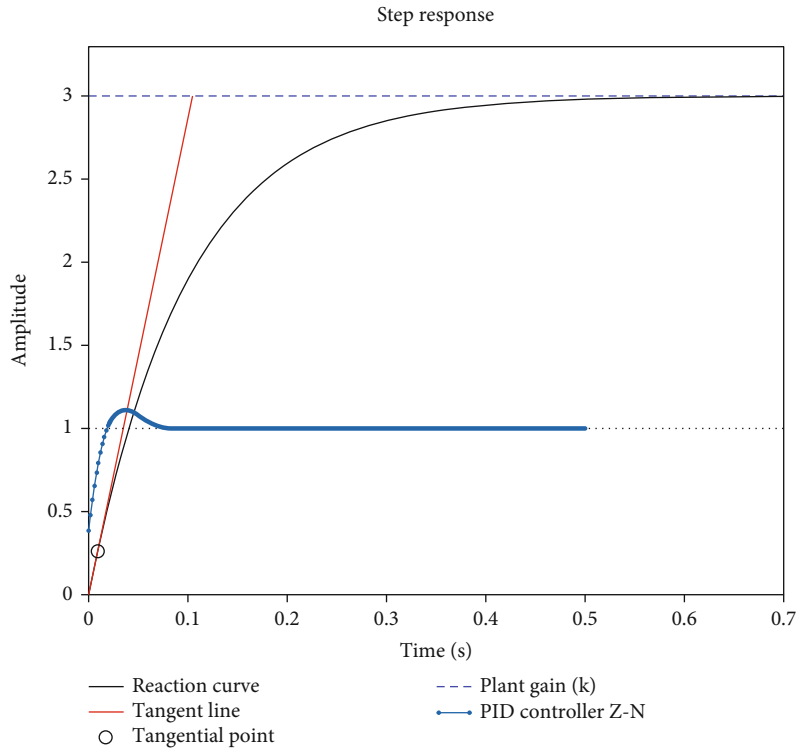

Figure 9: Reaction curve or a_{ref} tangent line in closed-loop PID-ZN (3).

33] and consequently instability in the system. The behavior of the acceleration response and vehicle speed, respectively, is shown in Figure 10.

The acceleration output signal initially presents an overshoot during the time of 0.1 s and an acceleration of 1.1 m/s^2 and a low stationary error; then, the system is controlled

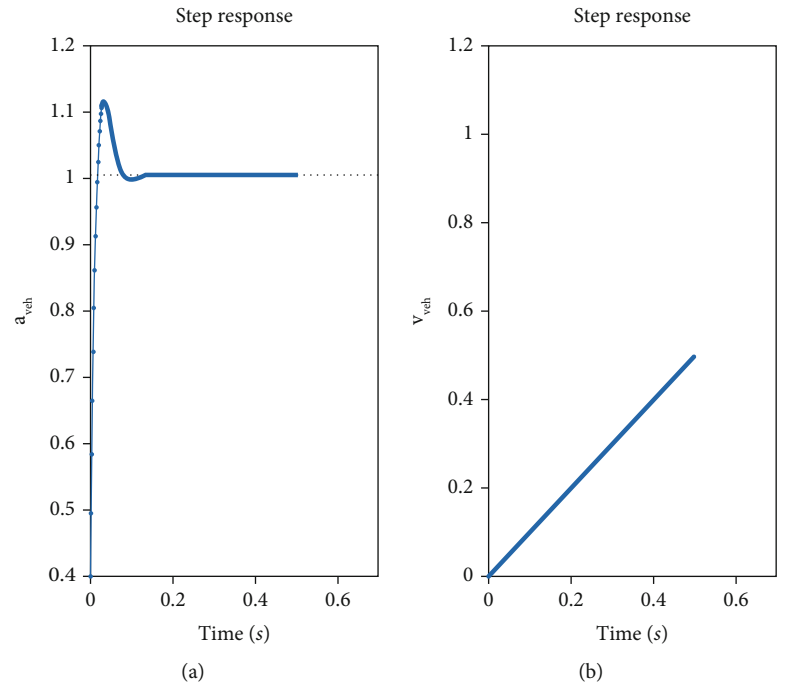

Figure 10: Acceleration (a) and vehicle speed (b), respectively, in closed-loop PID-ZN (3).

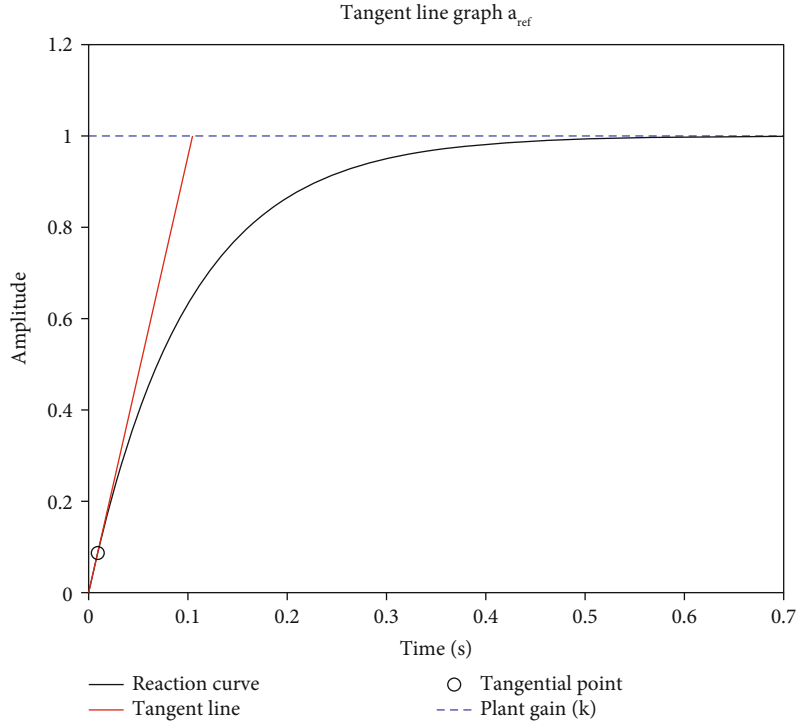

Figure 11: Reaction curve or a_{ref} tangent line in closed-loop PID-CHR (1).

[34]. The speed output signal relates to time, and each second tends to increase.

4.3. Minimum Plant Gain (CHR). The PID controller calculation is based on Table 3 proposed by Chien-Hrones-Reswick (CHR), where the PID controller gains are found, respectively, to be no response overshoot (0%); from Equation (3), the minimum plant gain $(K_{plant} = 1)$ was replaced together with the parameters of Tables 1 and 3 with the help of MATLAB software; the values of L, tau,

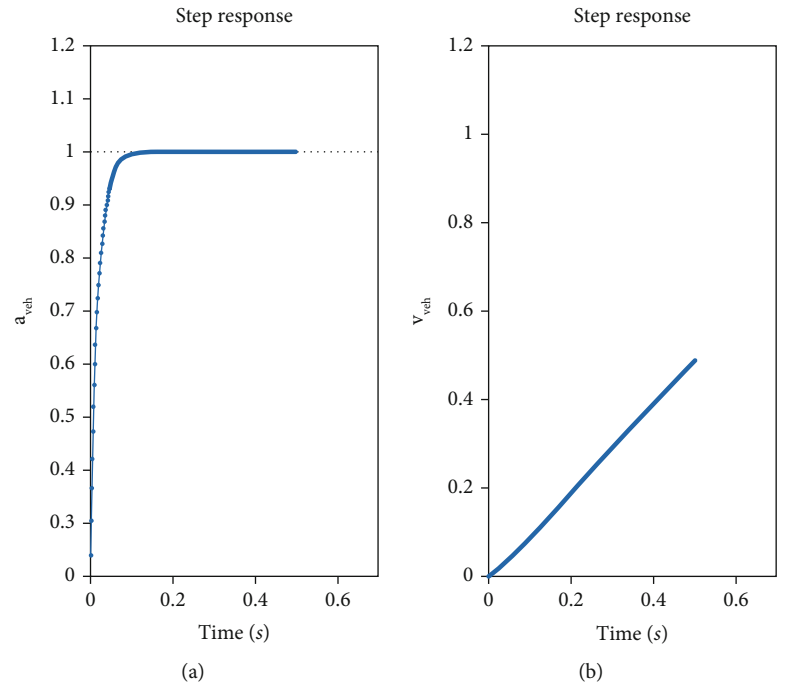

Figure 12: Vehicle acceleration (a) and speed (b) responses, respectively, in PID-CHR (1).

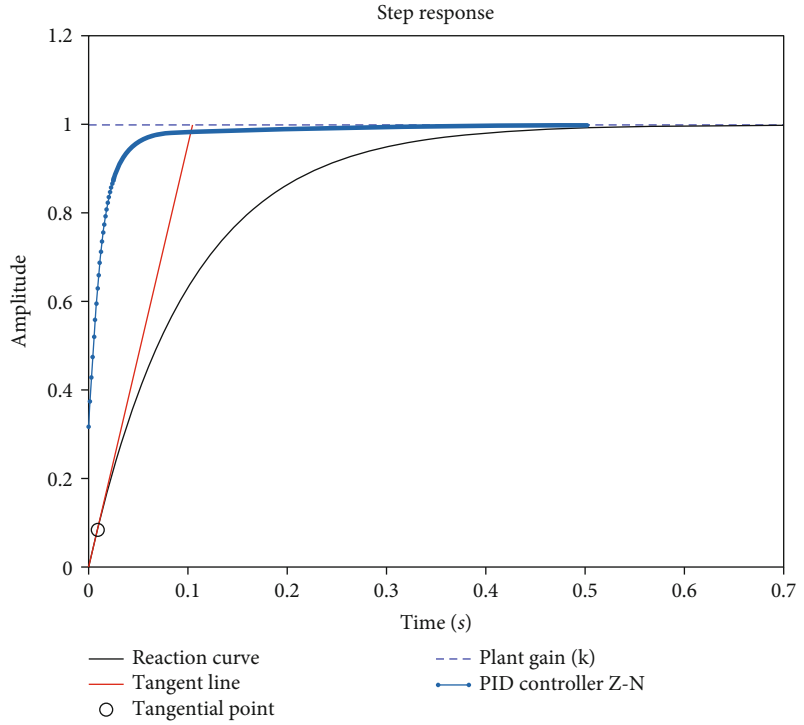

Figure 13: Reaction curve or a_{ref} tangent line in closed-loop PID-CHR (20%) (1).

and T are obtained; however, the PID controller is represented by

$$G_{P(s)} = \frac{0.003287s^2 + 0.7139s + 6.821}{0.1047s}. \quad (10)$$

The PID controller output can be evaluated by the reaction curve method; the system is excited by a step input signal, as shown in Figure 11.

The PID controller does not track input variables, which makes the system slow and uncontrolled; the behavior of the

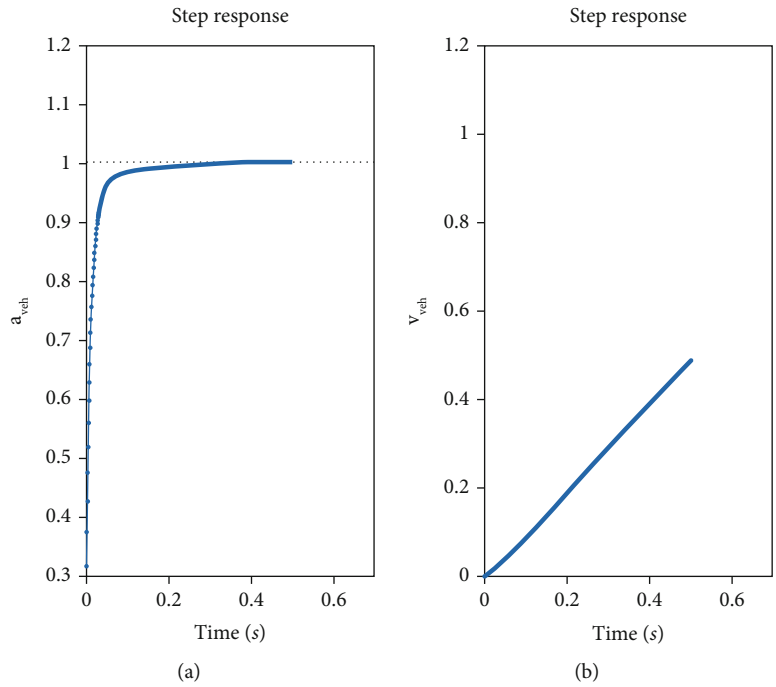

Figure 14: Vehicle acceleration (a) and speed (b) responses, respectively, in PID-CHR (20%) (1).

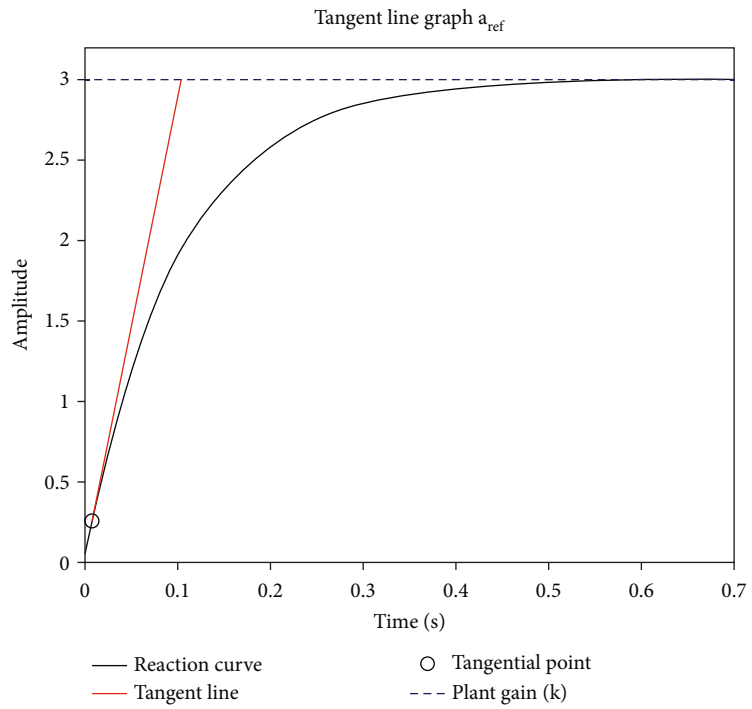

Figure 15: Reaction curve or a_{ref} tangent line in closed-loop PID-CHR (3).

acceleration response and vehicle speed, respectively, is shown in Figure 12.

The acceleration and velocity apparently have an adequate output, but in this case, the controller takes a long time to respond and this can cause instability in the system.

With 20% of the overshoot in response, the PID controller calculation is based on Table 3 proposed by Chien-Hrones-Reswick (CHR), where the PID controller gains are found, respectively. From Equation (3), the minimum plant gain $(K_{plant} = 1)$ was replaced together with the parameters

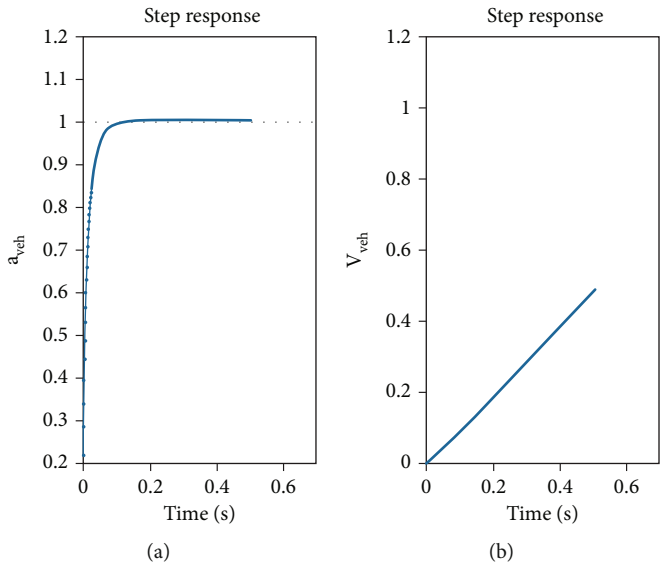

Figure 16: Vehicle acceleration (a) and speed (b) responses, respectively, in PID-CHR (3).

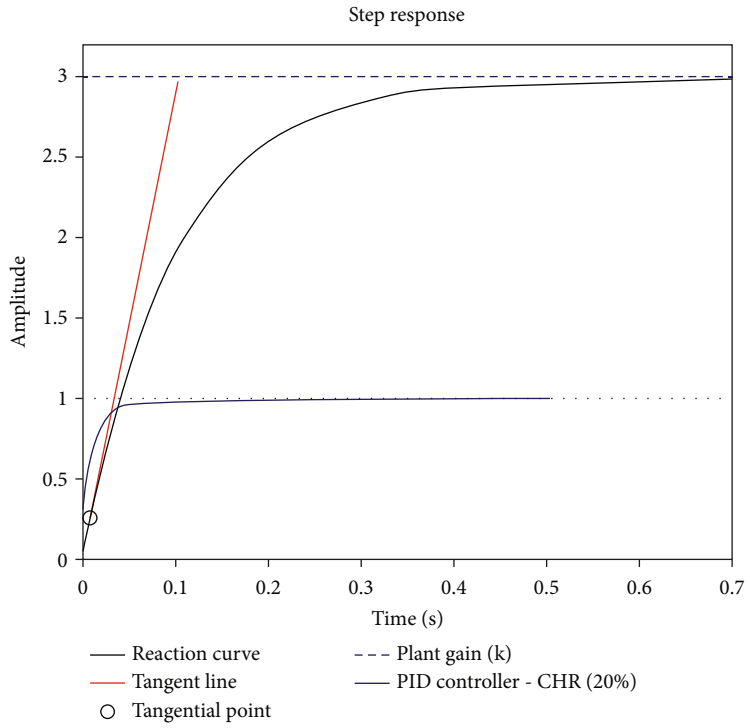

Figure 17: Reaction curve or a_{ref} tangent line in closed-loop PID-CHR (20%) (3).

of Tables 1 and 3 with the help of MATLAB software; the values of L, tau, and T are obtained; however, the PID controller is represented by

$$G_{P(s)} = \frac{0.006849s^2 + 1.583s + 10.8}{0.1465s}. \quad (11)$$

The PID controller output can be evaluated by the reaction curve method; the system is excited by a step input signal, as shown in Figure 13.

The output signal from the PID controller (reference acceleration) reaches the recommended gain; in this case, it does not produce a large stationary error and consequently stabilizes the system from the time of 0.28 s; the behavior of the acceleration response and vehicle velocity, respectively, is shown in Figure 14.

Acceleration response and velocity perform well, and this is due to the stable control of the system.

4.4. Maximum Plant Gain (CHR). The PID controller calculation is based on Table 3 proposed by Chien-Hrones-

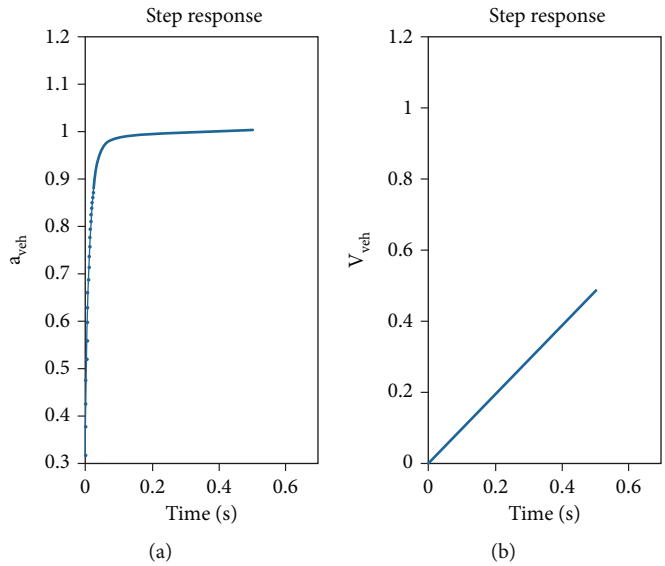

Figure 18: Vehicle acceleration (a) and speed (b) responses, respectively, in PID-CHR (20%) (3).

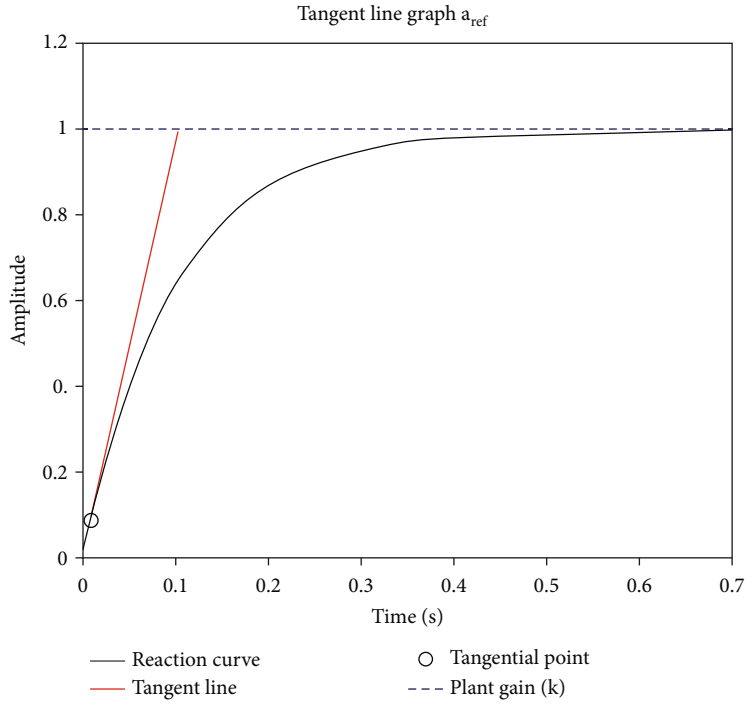

Figure 19: Reaction curve or a_{ref} tangent line in closed-loop PID-CC (1).

Reswick (CHR), where the PID controller gains are found, respectively, to be no response overshoot (0%); from Equation (3), the maximum plant gain ($K_{plant} = 3$) was replaced together with the parameters of Tables 1 and 3 with the help of MATLAB software; the values of L, tau, and T are obtained; however, the PID controller is represented by

$$G_{P(s)} = \frac{0.001096s^2 + 0.238s + 2.274}{0.1047s}. \quad (12)$$

The PID controller output can be evaluated by the reaction curve method; the system is excited by a step input signal, as shown in Figure 15.

The system was not controlled due to the fact that the PID controller output does not track its input in this sampling time; the behavior of the acceleration response and vehicle speed, respectively, is shown in Figure 16.

The acceleration and velocity apparently have an adequate output, but in this case, the controller takes a long time to respond and this can cause instability in the system.

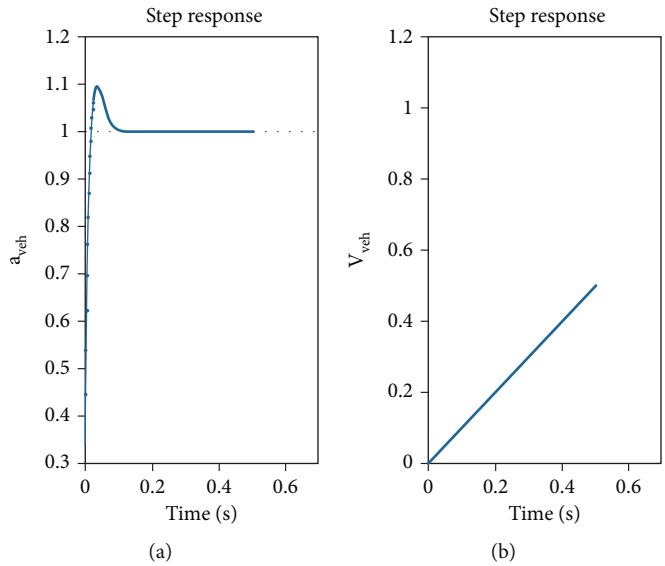

Figure 20: Vehicle acceleration (a) and speed (b) responses, respectively, in PID-CC (1).

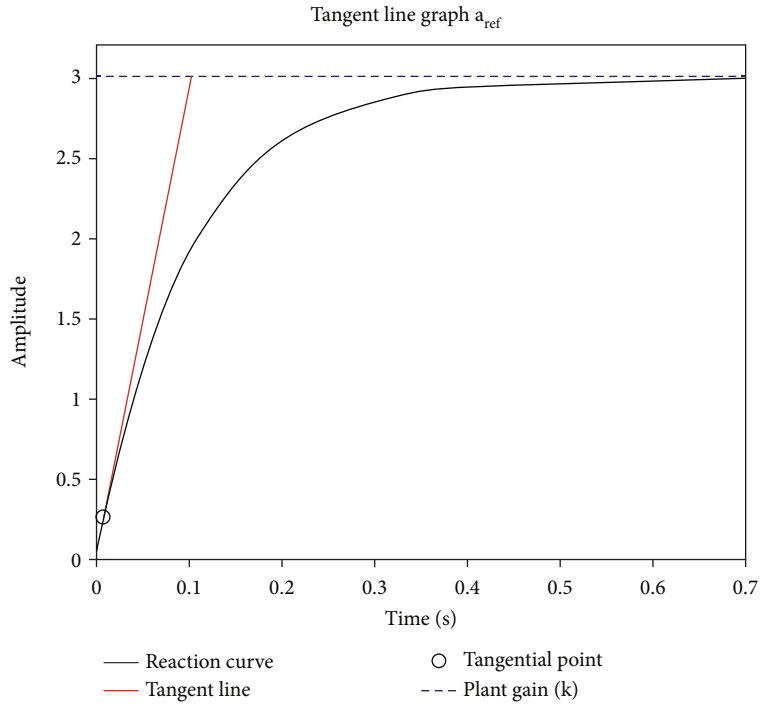

Figure 21: Reaction curve or a_{ref} tangent line in closed-loop PID-CC (3).

With 20% of the overshoot in response, the PID controller calculation is based on Table 3 proposed by Chien-Hrones-Reswick (CHR), where the PID controller gains are found, respectively. From Equation (3), the maximum plant gain ($K_{plant} = 3$) was replaced together with the parameters of Tables 1 and 3 with the help of MATLAB software; the values of L, tau, and T are obtained; however, the PID controller is represented by

$$G_{P(s)} = \frac{0.002283s^2 + 0.5275s + 3.6}{0.1465s}. \quad (13)$$

The PID controller output can be evaluated by the reaction curve method; the system is excited by a step input signal, as shown in Figure 17.

The PID controller (reference acceleration) does not reach the recommended gain, and it creates an interval

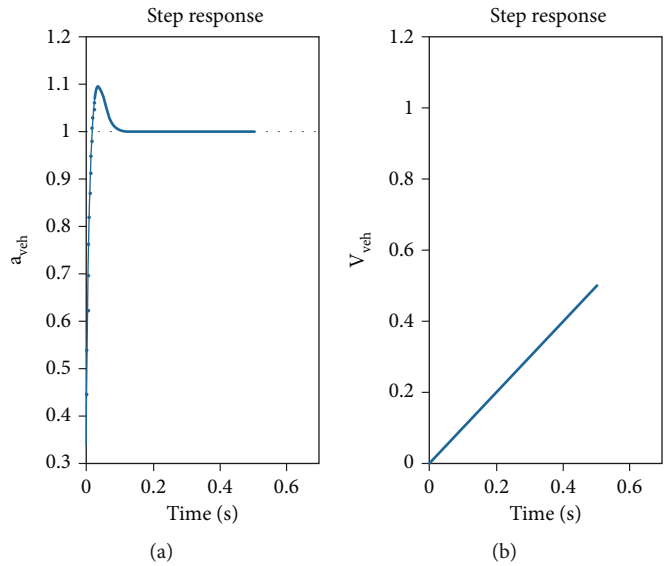

Figure 22: Vehicle acceleration (a) and speed (b) responses, respectively, in PID-CC (3).

Table 5: Transient response to a single-step entry.

PID controller	Overshoot M_O (%)	Settling time t_s (s)	Rise time t_r (s)	Peak amplitude
Ziegler-Nichols	11.100	0.073	0.015	1.110
Chien-Hrones-Reswick (20%)	0	0.128	0.035	0.999

between the input and output variables, which produces a large stationary error at all times; the system is not stable. The behavior of the acceleration response and vehicle velocity, respectively, is shown in Figure 18.

The system is not controlled; the controller takes a long time to respond. The acceleration and speed apparently have an adequate output.

4.5. Minimum Plant Gain (CC). The PID controller calculation is based on Table 4 proposed by Cohen-Coon (CC), where the PID controller gains are found, respectively. From Equation (3), the minimum plant gain ($K_{plant} = 1$) was replaced together with the parameters of Tables 1 and 4 with the help of MATLAB software; the values of L, tau, and T are obtained; however, the PID controller is represented by

$$G_{P(s)} = \frac{0.001161s^2 + 0.3466s + 15.59}{0.02223s}. \quad (14)$$

The PID controller output can be evaluated by the reaction curve method; the system is excited by a step input signal, as shown in Figure 19.

The system was not controlled because the PID controller does not track its input in this sampling time; the behavior of the acceleration response and vehicle speed, respectively, is shown in Figure 20.

For this sampling time, the PID controller response is slow, and this causes instability in the system.

4.6. Maximum Plant Gain (CC). From Equation (3), the maximum plant gain ($K_{plant} = 3$) was replaced together with the parameters of Tables 1 and 4 with the help of MATLAB software; the values of L, tau, and T are obtained; the PID controller is represented by

$$G_{P(s)} = \frac{0.0003871s^2 + 0.1155s + 5.196}{0.02223s}. \quad (15)$$

The PID controller output can be evaluated by the reaction curve method; the system is excited by a step input signal, as shown in Figure 21.

The system was not controlled because the PID controller output does not track its input in this sampling time. The behavior of the acceleration response and vehicle speed, respectively, is shown in Figure 22.

Apparently, the acceleration response and vehicle speed are great, and it is notable that the controller output takes a long time to respond (Figure 21), which makes the system uncontrollable.

5. Performance Index of the PID Controller

The Ziegler-Nichols and Chien-Hrones-Reswick (20%) tuning methods are the most indicated to be used in helping maneuver the vehicle system.

Some performance indexes, such as overshoot (M_O), settling time (t_s), and rise time (t_r), can evaluate the performance of the controller in the system. Table 5 shows the

performance of the tuning method of the PID controller based on the results of the simulations already highlighted.

These values were extracted from the PID controller response of Figure 7 (Ziegler-Nichols) and Figure 13 (Chien-Hrones-Reswick (20%)), both responses with minimum plant gain, that is, $K_{\text{plant}} = 1$. The performance index of the Ziegler-Nichols tuning method has an overshoot, a shorter settling time and a shorter rise time, and a greater amplitude than the desired amplitude it is considered. The performance index of the Chien-Hrones-Reswick (20%) tuning method has the opposite response, that is, desired amplitude, no overshoot, and larger settling and larger rise time. Both answers are acceptable because the PID controller showed stability even with time variation.

6. Discussion and Final Considerations

PI controller does not recognize its output variables to estimate its input values in order to have proper control of the vehicle system during the parking maneuver; the proposed PID controller guarantees stability in the system and classifies the operation action as robust according to the simulations presented, highlighting the 2 best tuning methods (ZN and CHR (20%)), both with minimal system gains (ZN method: aggressive tuning method but with tune adjustments, better control of the system achieved, and small values of settling time; CHR method (20% over value): faster system response with 20% over value and higher value requirement of settling time). However, the PID controller is recommended to control the parking maneuver assistance system integrated into the vehicle.

Data Availability

The data used to support the findings of this study are available from the corresponding author upon request.

Conflicts of Interest

The authors declare that there are no conflicts of interest regarding the publication of this paper.

Acknowledgments

The fourth author thanks CNPq for the financial support (Process: 310562/2021-0).

References

[1] Z. Yang, J. Huang, Z. Hu, D. Yang, and Z. Zhong, "Constraint-oriented integrated longitudinal and lateral robust control for connected and automated vehicle platoons," *Journal of Vibration and Control*, vol. 28, no. 5-6, pp. 593–605, 2022.

[2] C. M. Ionescu, E. H. Dulf, M. Ghita, and C. I. Muresan, "Robust controller design: recent emerging concepts for control of mechatronic systems," *Journal of the Franklin Institute*, vol. 357, no. 12, pp. 7818–7844, 2020.

[3] D. Xu, G. Wang, L. Qu, and C. Ge, "Robust control with uncertain disturbances for vehicle drift motions," *Applied Sciences*, vol. 11, no. 11, p. 4917, 2021.

[4] H. L. N. N. Thanh, N. X. Mung, N. P. Nguyen, and N. T. Phuong, "Perturbation observer-based robust control using a multiple sliding surfaces for nonlinear systems with influences of matched and unmatched uncertainties," *Mathematics*, vol. 8, no. 8, p. 1371, 2020.

[5] H. Liu, D. Liu, J. Xi, and Y. Yu, "Robust control for hypersonic vehicles with parametric and unstructured uncertainties," *Proceedings of the Institution of Mechanical Engineers, Part C: Journal of Mechanical Engineering Science*, vol. 232, no. 13, pp. 2369–2380, 2018.

[6] W. L. Torres, I. B. Q. Araujo, J. B. Menezes Filho, and A. C. Junior, "Mathematical modeling and PID controller parameter tuning in a didactic thermal plant," *IEEE Latin America Transactions*, vol. 15, no. 7, pp. 1250–1256, 2017.

[7] S. V. Samsonau, "Computer simulations combined with experiments for a calculus-based physics laboratory course," *Physics Education*, vol. 53, no. 5, article 055013, 2018.

[8] C. Imbert, "Computer simulations and computational models in science," in *Springer Handbook of Model-Based Science*, pp. 735–781, Springer, Cham, Switzerland, 2017.

[9] G. Q. Zeng, X. Q. Xie, M. R. Chen, and J. Weng, "Adaptive population extremal optimization-based PID neural network for multivariable nonlinear control systems," *Swarm and Evolutionary Computation*, vol. 44, pp. 320–334, 2019.

[10] W. Zheng, H. Wang, H. Wang, and S. Wen, "Dynamic output feedback control based on descriptor redundancy approach for networked control systems with multiple mixed time-varying delays and unmatched disturbances," *IEEE Systems Journal*, vol. 13, no. 3, pp. 2942–2953, 2019.

[11] J. Rüth, R. Glebke, K. Wehrle, V. Causevic, and S. Hirche, "Towards in-network industrial feedback control," in *Proceedings of the 2018 Morning Workshop on In-Network Computing*, pp. 14–19, Budapest Hungary, 2018.

[12] J. Li and Y. Niu, "Output-feedback-based sliding mode control for networked control systems subject to packet loss and quantization," *Asian Journal of Control*, vol. 23, no. 1, pp. 289–297, 2021.

[13] Y. Wang, M. Wei, X. Hu, M. Jiang, and L. Zhang, "Research on variable universe fuzzy PID control strategy of pipe lining induction heating system," *Modelling and Simulation in Engineering*, vol. 2020, Article ID 8852943, 9 pages, 2020.

[14] M. Huba, S. Chamraz, P. Bistak, and D. Vrancic, "Making the PI and PID controller tuning inspired by Ziegler and Nichols precise and reliable," *Sensors*, vol. 21, no. 18, p. 6157, 2021.

[15] K. S. Chia, "Ziegler-Nichols based proportional-integral-derivative controller for a line tracking robot," *Indonesian Journal of Electrical Engineering and Computer Science*, vol. 9, no. 1, pp. 221–226, 2018.

[16] N. Ahamad, S. Uniyal, A. Sikander, and G. Singh, "A comparative study of PID controller tuning techniques for time delay processes," *UPB Scientific Bulletin, Series C: Electrical Engineering and Computer Science*, vol. 81, no. 3, pp. 129–142, 2019.

[17] A. A. Hassan, N. K. Al-Shamaa, and K. K. Abdalla, "Comparative study for DC motor speed control using PID controller," *International Journal of Engineering and Technology*, vol. 9, no. 6, pp. 4181–4192, 2017.

[18] T. Suksawat and P. Kaewpradit, "Comparison of Ziegler-Nichols and Cohen-Coon tuning methods: implementation to water level control based MATLAB and Arduino," *Engineering Journal Chiang Mai University*, vol. 28, no. 1, pp. 153–168, 2021.

[19] F. Isdaryani, F. Feriyonika, and R. Ferdiansyah, "Comparison of Ziegler-Nichols and Cohen Coon tuning method for magnetic levitation control system," *Journal of Physics: Conference Series, IOP Publishing*, vol. 1450, no. 1, article 012033, 2020.

[20] V. Dubey, H. Goud, and P. C. Sharma, "Role of PID control techniques in process control system: a review," *Data Engineering for Smart Systems*, pp. 659–670, 2022.

[21] H. Du, P. Liu, Q. Cui, X. Ma, and H. Wang, "PID controller parameter optimized by reformative artificial bee colony algorithm," *Journal of Mathematics*, vol. 2022, Article ID 3826702, 16 pages, 2022.

[22] O. Briones, R. Alarcón, A. J. Rojas, and D. Sbarbaro, "Tuning generalized predictive PI controllers for process control applications," *ISA Transactions*, vol. 119, pp. 184–195, 2022.

[23] R. De Keyser, C. I. Muresan, and C. M. Ionescu, "Universal direct tuner for loop control in industry," *IEEE Access*, vol. 7, pp. 81308–81320, 2019.

[24] A. Kaveh and T. Bakhshpoori, *Metaheuristics: Outlines, MATLAB Codes and Examples*, Springer International Publishing, Cham, Switzerland, 2019.

[25] Y. Xue, Y. Guo, Y. Shi, L. Z. Lv, and H. D. He, "Feedback control for the lattice hydrodynamics model with drivers' reaction time," *Nonlinear Dynamics*, vol. 88, no. 1, pp. 145–156, 2017.

[26] J. Li and Y. T. Chen, *Computational Partial Differential Equations Using MATLAB®*, CRC Press, 2019.

[27] P. S. Bokare and A. K. Maurya, "Acceleration-deceleration behaviour of various vehicle types," *Transportation Research Procedia*, vol. 25, pp. 4733–4749, 2017.

[28] W. Rui, S. Qiuye, Z. Pinjia, G. Yonghao, Q. Dehao, and W. Peng, "Reduced-order transfer function model of the droop-controlled inverter via Jordan continued-fraction expansion," *IEEE Transactions on Energy Conversion*, vol. 35, no. 3, pp. 1585–1595, 2020.

[29] G. Q. Carapia and I. Markovsky, "Input parameters estimation from time-varying measurements," *Measurement*, vol. 153, article 107418, 2020.

[30] S. Kakkar, T. Maity, R. K. Ahuja et al., "Design and control of grid-connected PWM rectifiers by optimizing fractional order PI controller using water cycle algorithm," *IEEE Access*, vol. 9, pp. 125941–125954, 2021.

[31] S. Oladipo, Y. Sun, and Z. Wang, "Optimization of PID controller with metaheuristic algorithms for DC motor drives: review," *The International Review of Electrical Engineering*, vol. 15, no. 5, pp. 352–381, 2020.

[32] F. O. Silva, L. P. S. Paiva, and G. S. Carvalho, "Error analysis of accelerometer- and magnetometer-based stationary alignment," *Sensors*, vol. 21, no. 6, p. 2040, 2021.

[33] J. Li and T. Li, "Time-varying additive model with autoregressive errors for locally stationary time series," *Communications in Statistics-Theory and Methods*, vol. 2021, pp. 1–31, 2021.

[34] J. Sanchez, M. Guinaldo, A. Visioli, and S. Dormido, "Enhanced event-based identification procedure for process control," *Industrial and Engineering Chemistry Research*, vol. 57, no. 21, pp. 7218–7231, 2018.